Geomechanics and Engineering, *Vol. 13, No. 1 (2017) 79-97*
DOI: https://doi.org/10.12989/gae.2017.13.1.079

Application of a modified structural clay model considering anisotropy to embankment behavior

Hao Zhang [1a], Qiushi Chen [2b], Jinjian Chen [1c] and Jianhua Wang [*1]

[1] *Department of Civil Engineering, Shanghai Jiao Tong University, Shanghai, 200240, China*
[2] *Glenn Department of Civil Engineering, Clemson University, Clemson, SC 29634, USA*

(*Received January 25, 2016, Revised March 31, 2017, Accepted February 16, 2017*)

Abstract. Natural clays exhibit features such as structural and anisotropy. In this work, a constitutive model that is able to replicate these two salient features of natural clays is presented. The proposed model is based on the classical S-CLAY1 model, where the anisotropy of the soil is captured through the initial inclination and rotation of the yield surface. To account for the structural of the soil, the compression curve of the reconstituted soil is taken as the reference. All parameters of the proposed constitutive model have clear physical meanings and can be conveniently determined from conventional triaxial tests. This proposed model has been used to simulate the behavior of soft soil in the undrained triaxial tests and the performance of Murro embankment in terms of settlement and horizontal displacements during embankment construction and consolidation stage. Results of numerical simulations using proposed model have been compared with the field measurement data. The comparisons show that the two features significantly influence the prediction results.

Keywords: constitutive model; structural; anisotropy; soft clay; embankment

1. Introduction

Construction of embankment on soft soil has seen a considerable increase due to economic and societal development in recent years (Leroueil and Vaughan 1990). As the influence of fundamental features such as anisotropy and structural, the stress-strain behavior of soft soil is very complex and highly nonlinear. Predicting the behavior of embankment on soft soil remains a major challenge in geotechnical engineering.

Anisotropy of natural soil is developed during the long-term sedimentation, which greatly affects its mechanical behavior. Neglecting such effect may greatly undermine the accuracy of predicted behavior (Zdravkovic *et al*. 2002). To this end, a variety of constitutive models accounting for plastic anisotropy of natural soils have been developed (Dafalias 1986, Whittle and Kavvadas 1994, Marcin and Pieter 2004). The S-CLAY1 model (Wheeler *et al*. 2003) introduces a rotational hardening component to account for the influence of plastic anisotropy in soft clays. The rotational hardening law of this model includes dependence on plastic shear strain increment as

*Corresponding author, Professor, E-mail: wjh417@163.com
[a] Ph.D., E-mail: zhanghao800329@163.com
[b] Ph.D., E-mail: qiushi@clemson.edu
[c] Ph.D., E-mail: chenjj@sjtu.edu.cn

well as plastic volumetric strain increment. Based on the S-CLAY1 model, Yin (Karstunen and Yin 2010) proposed an elasto-viscoplastic model EVP-SCLAY1S, which is able to account for time-dependent large strain anisotropy, bonding and structural of naturally clays. And the model has been applied to simulate the behavior of Murro clay.

Generally, the natural soils exhibit higher strength than the reconstituted soils at the same void ratio. The difference has been attributed to the structural of soils (Locat and Lefebvre 1985, Burland 1990, Cotecchia and Chandler 2000, Nakano *et al*. 2005, Ng *et al*. 2011, Yin 2012, Chen *et al*. 2014). Experiment studies (Burland 1990, Leroueil and Vaughan 1990, Vincenzo and Ghassan 2009, Cheng and Wang 2016) show that when natural soils are compressed, the structural is progressively lost and soil starts to behave as a reconstituted soil. Great progress has been made in recent years to account for the behavior of soil with natural structural in constitutive models (Leroueil *et al*. 1979). Based on the MCC (Modified Cam Clay) model, Chai *et al*. (2004) introduced structural-dependent compression behavior and discussed the effects of structural on the calculated load-settlement curve. Liu and Carter (2002) and John *et al*. (2005) introduced a simple predictive model for naturally structural clay. The model incorporated the effect of structural on the volumetric deformation behavior and the plastic strain direction into the MCC model. The effect of structural on volumetric deformation is taken into account by a parameter called additional void ratio. Based on an intrinsic yield surface proposed by Gens and Nova (1993), Karstunen *et al*. (2005) developed an S-CLAY1S model for structural soils. Kimoto and Oka (2005) developed a rate-dependent model accounting for structural and inherent anisotropy.

In this study, an anisotropic plasticity model for clays that is able to account for structural is developed. The model is extended from the classical S-CLAY1 model (Wheeler *et al*. 2003), the initial and induced anisotropy is expressed through the initial inclination and subsequent rotation of the yield surface. The structural effect was expressed through the exponential function of Δe (the additional void ratio between the structural soil and reconstituted soil) (Jirayut *et al*. 2010).

The proposed model is then implemented into a finite element code and is used to simulate undrained triaxial tests and Murro test embankment in terms of settlement and horizontal displacement. The results of the numerical analyzes are compared with the experimental results and field dates to demonstrate the applicability of the proposed model and the effects of anisotropy and structural on predicted behavior.

2. Formulation of the constitutive model

2.1 Description of anisotropy

The starting point of the proposed constitutive model is the S-CLAY1 model (Wheeler *et al*. 2003). The yield surface of S-CLAY1 model is a sheared ellipse in p'-q space, as shown in Fig. 1.

The inclination of the yield curve is described with a scalar parameter α, which is identical to that proposed by Dafalias (1987)

$$f = (q - \alpha p')^2 - (M^2 - \alpha^2)(p_m' - p')p' = 0 \tag{1}$$

Where M is the stress ratio η (= q/p') at the critical state. There are two internal variables in the S-CLAY1 model, i.e., p'_m and α, which control the size and inclination of the yield surface respectively. The parameter α is a measure of the degree of plastic anisotropy of the soil. For isotropic behavior, $\alpha = 0$ and Eq. (1) reduces to the Modified Cam Clay (MCC) yield surface.

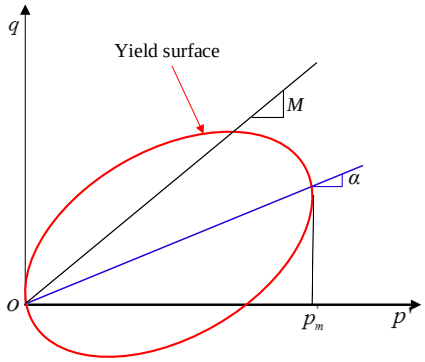

Fig. 1 S-CLAY1model yield surface

S-CLAY1 model incorporates two hardening laws describing the evolution of two internal variables. The first hardening law, which is the same as that in the MCC model, describes changes in the size of the yield surface (dp'_m) caused by changes of plastic volumetric strain $d\varepsilon_v^p$

$$dp'_m = \frac{vp'_m d\varepsilon_v^p}{\lambda - \kappa} \tag{2}$$

where λ is the slope of the post-yield compression curve for a constant η stress path involving no change of anisotropy (α = constant) and κ is the slope of elastic swelling lines.

The second hardening law describes changes in the inclination of the yield surface associated with changes in plastic volumetric strain and shear strain:

$$d\alpha = \mu\left[\left(\frac{3\eta}{4} - \alpha\right)\left\langle d\varepsilon_v^p \right\rangle + \beta\left(\frac{\eta}{3} - \alpha\right)\left|d\varepsilon_s^p\right|\right] \tag{3}$$

where the parameter μ controls the rate at which the components of the deviatoric fabric tensor moves toward their current target values, which depends on the stress path. Parameter β controls the relative effect of plastic shear strain in rotating the yield and loading surfaces, the parameters β can be expressed by (Wheeler *et al*. 2003)

$$\beta = \frac{3(4M^2 - 4\eta_{K_0}^2 - 3\eta_{K_0})}{8(\eta_{K_0}^2 - M^2 + 2\eta_{K_0})} \tag{4}$$

The expression of the control parameter μ can be obtained from (Sheng *et al*. 2000)

$$\mu = \frac{2\beta(1+e_0)}{\lambda_n - \kappa}\ln\frac{10M^2 - 2\alpha_0\beta}{M^2 - 2\alpha_0\beta} \tag{5}$$

To interpolate M between its values M_c (for compression) and M_e (for extension), a modification of M by means of the Lode angle θ is assumed (Sheng *et al*. 2000)

$$M = M_c\left(\frac{2c^4}{1 + c^4 - (1 - c^4)\sin 3\theta}\right)^{1/4} \tag{6}$$

in which

$$c = M_e / M_c \tag{7}$$

$$\frac{-\pi}{6} \le \theta = \frac{1}{3}\sin^{-1}\left(\frac{-3\sqrt{3}J_3}{2J_2^{3/2}}\right) \le \frac{\pi}{6} \tag{8}$$

where J_2 and J_3 are the second and the third invariants of the deviatoric stress tensor, respectively.

Table 1 Selected approaches to account for soil structural in current constitutive models

Models	Internal variables for structural	Key parameters	Comments
Gajo and Wood 2001	$dr = -\frac{k}{\lambda-\kappa}(r-1)^{\psi} d\varepsilon_d^p$ $d\varepsilon_d^p = \sqrt{(1-A)(d\varepsilon_v^p)^2 + A(d\varepsilon_s^p)^2}$	r is a variable describing the current degree of cementation. k and ψ are structural control parameters. ε_d^p is the generalized plastic strain.	Consider the influence of both plastic volumetric strain and plastic shear strain. Parameter k and ψ cannot be determined in a direct way.
Liu and Carter 2002	$\Delta e = \Delta e_i \left(\frac{p'_{yi}}{p'_s}\right)^b$	Δe is the additional void ratio, i.e., the difference in void ratio between natural and reconstituted soil at same confining stress. b is the structural control parameter.	Back analysis is needed to determine the parameter b. The influence of plastic shear strain is not considered.
Marcin and Pieter 2004	$b^k = b_0^k \exp\left(-a\left\|\varepsilon_n^{pk}\right\|\right)$	b^k is the state variable representing bonding, a is the control parameter, ε_n^{pk} is the normal invariant of plastic micro strain.	The determination of parameter a is very difficult, and the simulation result is very sensitive to this parameter. The influence of plastic shear strain is not considered.
Koskinen *et al.* 2002	$d\chi = -a\chi\left(\left\|d\varepsilon_v^p\right\| + b\left\|d\varepsilon_s^p\right\|\right)$	χ is the amount of bonding, constant a controls the absolute rate of destructuration and b controls relative rate of structuration	Parameters a and b are fitting parameters without clearn physical meanings.
Kavvadas and Amorosi 2000	$da = a\left[\left\{\left(\frac{1+e}{\lambda-\kappa}\right) - \zeta_v \exp(-\eta_v, \varepsilon_v^p)\right\}\right.$ $\left. d\varepsilon_v^p + \left\{\theta_q - \zeta_q \exp(-\eta_q, \varepsilon_s^p)\right\} d\varepsilon_s^p\right]$	Parameter a represents the size of the yield surface of structural soil. (ζ_v, η_v) are the volumetric structural degradation parameter, and (θ_q, ζ_q, η_q) are deviatoric structural degradation parameters.	This model contains more fitting parameters and are difficult to determine in calibration process.

2.2 Proposed description of structural

Based on the MCC (Modified Cam Clay) model, taking the yield surface of reconstituted soil as reference, many different constitutive models have been proposed to account for the influence of structural. The approaches to incorporate structural of these models are summarized in Table 1.

In this study, based on the destructuration law proposed by Liu and Carter (2002), a new direct method to determine the structural parameters is proposed, which incorporates the influence of plastic shear strain on the structural, as well be detailed in the following.

Taking the compression curve of reconstituted soils as reference, Liu and Carte (2000) proposed the use of the additional void ratio (Δe) to represent the difference between the structural (natural) soil and its corresponding reconstituted soil. Δe decreases with the increase of stress and will eventually diminish at a very high stress, as shown in Fig. 2(b). The yield surface for structural and corresponding reconstituted soil is shown in Fig. 2(a).

The compression behavior during the destructuring process of structural soil can be equivalently captured by describing the change in the void ratio, i.e.,

$$e = e^* + \Delta e \tag{9}$$

where e is the void ratio of structural soil, e^* is the void ratio of reconstituted clay at the same stress state and can be expressed as

$$e^* = e^*_{IC} - \lambda^* \ln p' \tag{10}$$

where e^*_{IC} is the void ratio at a reference mean effective stress on the compression line of a reconstituted soil. For instance, e^*_{IC} can be approximately taken as the initial void ratio of corresponding natural clay, λ^* is the slope of the compression line of reconstituted soil.

The void ratio e for a structural soil can be expressed in terms of the corresponding void ratio for the reconstituted soil e^*, the additional void ratio Δe as (Liu and Carter 2000)

$$e = e^* + \Delta e = e^* + \Delta e_i \left(\frac{p'_{yi}}{p'} \right)^b \tag{11}$$

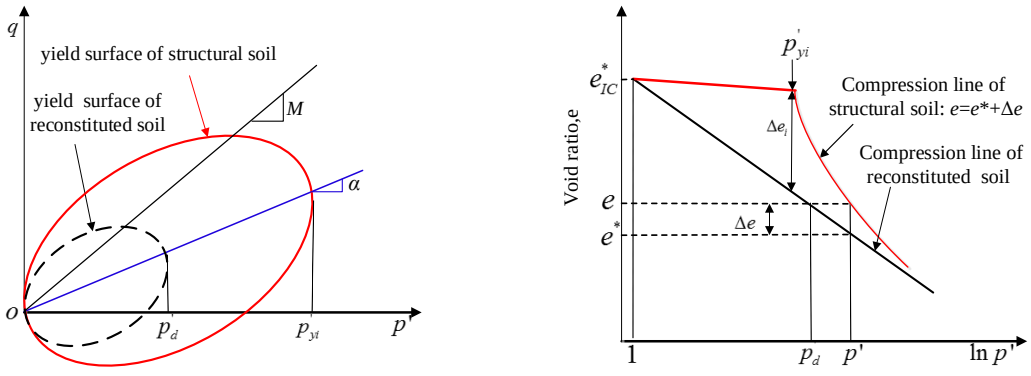

Fig. 2 Material idealization of structural soil: (a) Yield surfaces for structural soil and reconstituted soil; (b) One-dimensional compression behavior of structural soil showing the additional void ratio (Δe)

where p'_{yi} is the yield stress and p' is the current mean stress, b is called the structural index due to volumetric deformation. At the yield point, the increment of void ratio increment for a structural soil (de) and reconstituted soil (de*) can be expressed as

$$de = -\frac{\lambda_n}{p'_{yi}} dp' \tag{12}$$

$$de^* = -\frac{\lambda^*}{p'_{yi}} dp' \tag{13}$$

Combining Eqs. (11), (12) and (13), parameter b can be obtained and it is written as

$$b = \frac{\lambda_n - \lambda^*}{\Delta e_i} \tag{14}$$

In the proposed model, it is assumed that the yield surface of reconstituted soil has the same shape as the yield surface of structural soil. p'_d and p' represent the size of yield surface for reconstituted soil and structural soil, respectively, they can be related through the parameter Δe

$$p' = p'_d \exp\left(\frac{\Delta e}{\lambda^* - \kappa}\right) \tag{15}$$

where the additional void ratio Δe serves as a structural parameter and its initial value Δe_i can be determined from one-dimensional conventional compression tests, as shown in Fig. 2. The value of Δe decreases with the development of plastic deformation.

Eq. (15) depicts the relationship between the strucutral parameter Δe and the corresponding effective stress p'. The value of Δe is changing owing to structural degradation, ultimately to zero, analogously to the S-CLAY1S model (Karstunen *et al*. 2005).

$$d(\Delta e) = -\xi \Delta e \left(\left| d\varepsilon_v^p \right| + \xi_d d\varepsilon_s^p \right) \tag{16}$$

Where ξ and ξ_d are structural parameters, in which parameter ξ controls the absolute rate of destructuration and ξ_d controls relative effectiveness of plastic deviatoric strains and plastic volumetric strain in destroying the bonding. In this study, an approach to determine these two structural parameters is proposed as follows.

Under isotropic compression condition, the plastic shear strain is zero. When the effective stress p' is greater than the yield stress p'_{yi}, the bonding parameter increment $d(\Delta e)$ of structural soil can be expressed as (see Fig. 3)

$$d(\Delta e) = de_n^p - de_r^p = (1 + e_0)\left(\frac{\lambda_n - \lambda^*}{\lambda_n - \kappa}\right) d\varepsilon_v^p \tag{17}$$

Where de_n^p and de_r^p is the plastic void ratio increment of structural soil and reconstituted soil, respectively. Let $\xi = (1 + e_0)(\lambda_n - \lambda^*)/(\lambda_n - \kappa)$, then the Eq. (17) can be written as

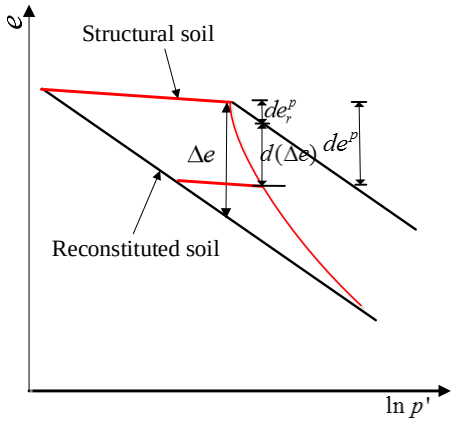

Fig. 3 Isotropic compression curves

$$d\left(\Delta e\right)=\xi d\varepsilon_v^p \tag{18}$$

Parameter ξ_d can be determined from a one-dimensional compression test, for the one-dimensional compression test, the initial inclination angle α remains constant, i.e., $\alpha = \alpha_{K0}$. The relationship $d\varepsilon_s^p / d\varepsilon_v^p$ can be derived as

$$\frac{d\varepsilon_s^p}{d\varepsilon_v^p}=\frac{2(\eta_{K0}-\alpha_{K0})}{M^2-\eta_{K0}^2} \tag{19}$$

Where η_{K0} is the stress ratio of the one-dimension compression test, which can be written as

$$\eta_{K0}=3\left(1-K_0\right)/\left(1+2K_0\right) \tag{20}$$

The void ratio increment $d(\Delta e)$ can be expressed from Eq. (11)

$$d\left(\Delta e\right)=-\frac{b\Delta e}{p'}dp' \tag{21}$$

Combined with Eqs. (16), (19) and (21), it can be obtained that

$$\xi\left(\lambda_n-\kappa\right)\left(M^2-\eta_{K0}^2+2\xi_d(\eta_{K0}-\alpha_{K0})\right)=b\left(1+e_0\right)\left(M^2-\eta_{K0}^2\right) \tag{22}$$

In the above analysis, parameter ξ can be expressed as

$$\xi=(1+e_0)(\lambda_n-\lambda^*)/(\lambda_n-\kappa) \tag{23}$$

Combined with Eqs. (22) and (23), the expression of parameter ξ_d can be obtained

$$\xi_d=\frac{\left(M^2-\eta_{K0}^2\right)\left(b+\lambda^*-\lambda_n\right)}{2(\eta_{K0}-\alpha_{K0})\left(\lambda_n-\lambda^*\right)} \tag{24}$$

Table 2 State parameters and soil constants of this model

Group	Parameter	Definition	Determination
Modified Cam Clay parameters	p_{yi}	Initial size of yield surface	From consolidation test on structural soil
	e_0	Initial void ratio	Standard manner from undisturbed sample
	ν	Poisson′s ratio	Typically (0.15-0.35)
	κ	Slope of the swelling line	From consolidation test
	λ_n	Slope of the compression line of structural soil	From consolidation test on intact sample
	λ^*	Slope of the intrinsic compression line	From consolidation test on reconstituted sample
	M	Slope of the critical state line	From triaxial shear test in compression
Structural parameters	Δe_i	Additional void ratio	From one consolidation test on structural soil and one isotropic consolidation test on reconstituted soil
	ξ	Absolute rate of bond degradation	From oedometer test and i otropic consolidation or Eq. (23)
	ξ_d	Relative rate of bond degradation	From oedometer test and isotropic consolidation or Eq. (24)
Anisotropy parameter	α_0	Initial inclination angle of yield surface	From one-dimensional consolidation test
	μ	Absolute rate of yield surface rotation	From Eq. (5)
	β	Relative rate of yield surface rotation	From Eq. (4)

Considering the influence of structural, the yield surface equation can be expressed as

$$f = (q - \alpha p')^2 - (M^2 - \alpha^2)\left(p'_{yi}\left(\frac{\Delta e_i}{\Delta e}\right)^{1/b} - p' \right) p' = 0 \tag{25}$$

The material constants and state variables in the proposed model can be classified into three groups, which are summarized in Table 2.

This proposed model has been implemented into the finite element code ABAQUS as a user-material soil model. By switching on/off certain parameters, this proposed model can be reduced to only consider anisotropy ($\Delta e_i = \xi = \xi_d = 0$) or structural ($\alpha_0 = \mu = \beta = 0$), which can also be reduced to Modified Cam Clay (MCC) ($\alpha_0 = \mu = \beta = 0$ and $\Delta e_i = \xi = \xi_d = 0$).

3. Model parameters and element test

3.1 Determination of the structural parameter

It can be seen from Eq. (24) that the structural parameter ξ_d can be directly related to the

Table 3 Calculate of parameter b for 8 structural soils

Clay	λ_n	λ^*	κ	Δe_i	p'_{yi} (kPa)	$b = (\lambda_n - \lambda^*)/\Delta e_i$
Bothkennar	0.44	0.23	0.028	0.39	55	0.53
Sault Ste Marie	0.31	0.14	0.021	0.25	98	0.68
Troll	0.34	0.13	0.022	0.35	190	0.60
Pisa	0.42	0.26	0.07	0.35	155	0.45
Osaka	0.31	0.21	0.04	0.21	185	0.47
Lianyungang	0.30	0.21	0.04	0.47	65	0.19
Wenzhou	0.49	0.20	0.04	0.53	140	0.54
Shanghai	0.17	0.09	0.01	0.17	45	0.47

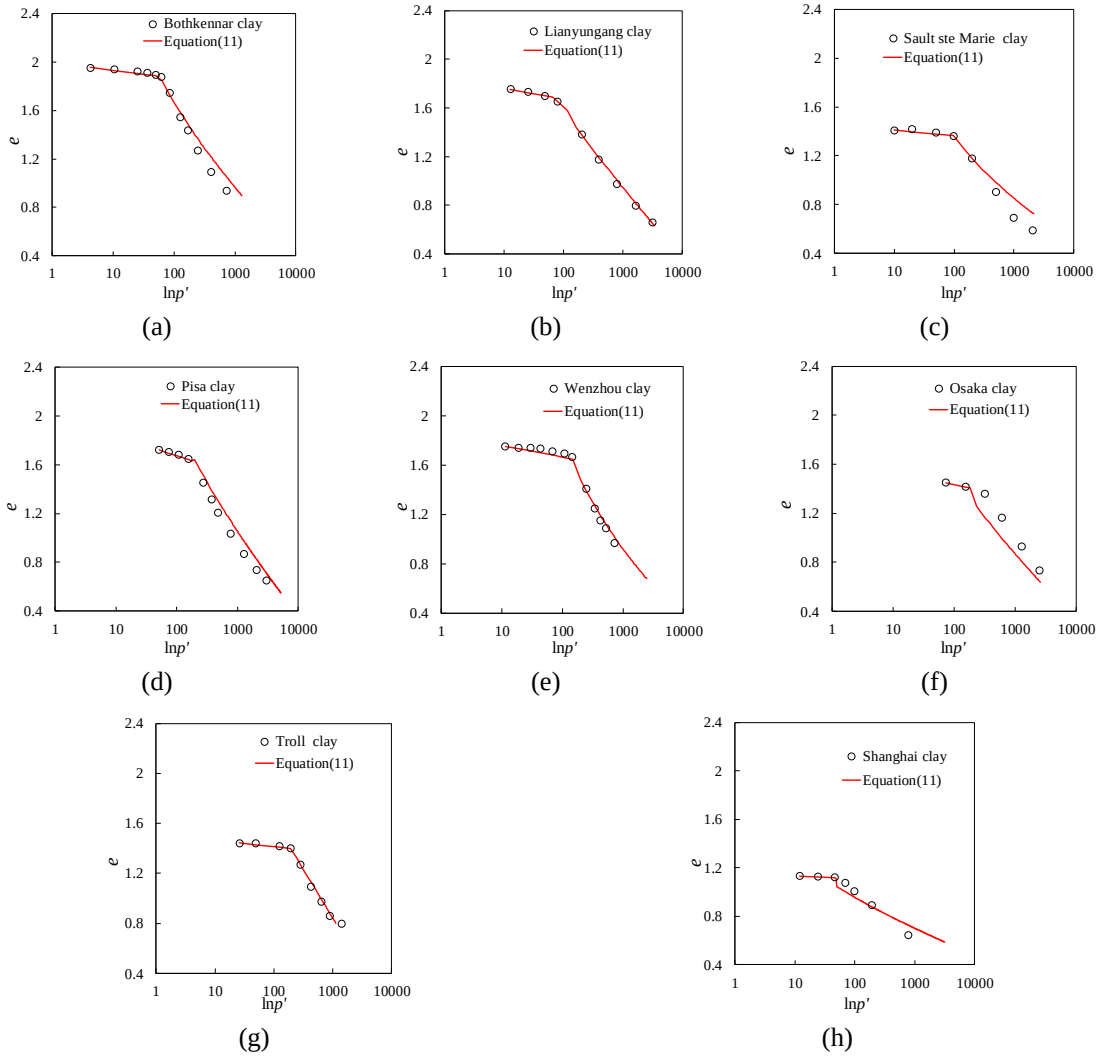

Fig. 4 Compression curves for 8 structural clays: (a) Bothkennar clay; (b) Lianyungang clay; (c) Sault ste Marie clay; (d) Pisa clay; (e) Wenzhou clay; (f) Osaka clay; (g) Troll clay; (h) Shanghai clay

parameter *b*, which has a clear physical meaning and controls the shape of the compression curve of structural soil. The parameter *b* can be easily calculated using Eq. (11). To illustrate this point, consolidation test data for 8 structural soil samples are collected from the literatures (Yin 2012, Nakano *et al*. 2005, Ng *et al*. 2011) and the parameter *b* is calculated and used to simulate the compression curve for the 8 structural soils according to Eq. (11). The values of compression parameters are listed in Table 3.

Fig. 4 shows the comparisons between the simulated results with Eq. (11) and the experiment results. It can be seen that for the structural clay, there is an obvious yield point for the compression curve. The simulated results agree well with the experiment results when the parameter *b* of Eq. (14) is adopted. The curve fitting is not needed to determine the structural parameter *b* as the original model proposed by Liu and Carter (2002), which simplify the calibration process.

3.2 Triaxial tests on soft clays

In this section, the proposed constitutive model is employed to simulate the behavior of Vallericca clay (Burland *et al*. 1996) and Shangai clay (Huang *et al*. 2011) in triaxial compression tests. The values of input parameters of the two clays are listed in Table 4.

The triaxial drained test on Shanghai soft clay was carried out by Huang *et al*. (2011). The samples were anisotropically consolidated to their in-situ stress states. In the shearing stage, the specimens were loaded in drained condition following different stress paths, which are represented by the angle between stress path and p'-axis in the p-q plane, Fig. 5 shows the loading stress paths, the experimental results of SCD50 and SED56 have been selected to compare with the simulated results.

Fig. 6 shows the simulated triaxial compression test results with the angle between stress path and p'-axis being 50 degree. It can be seen that the simulation using proposed constitutive model

Table 4 Model parameters for Vallericca and Shanghai clays

Clay	λ_n	λ^*	κ	M	ν	e_0	p'_{yi} (kPa)	ξ	ξ_d	Δe_i
Vallericca	0.148	0.124	0.022	0.9	0.2	0.84	1800	0.35	11.0	0.12
Shanghai	0.21	0.11	0.04	1.28	0.2	1.40	90	1.41	2.08	0.45

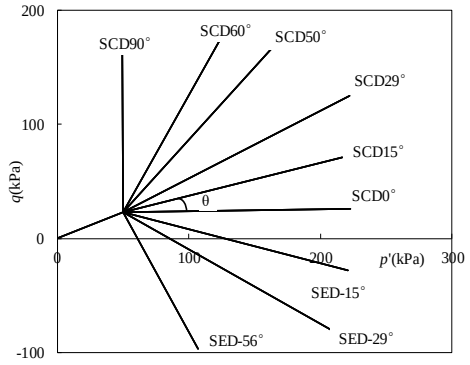

Fig. 5 Standard consolidation stress paths

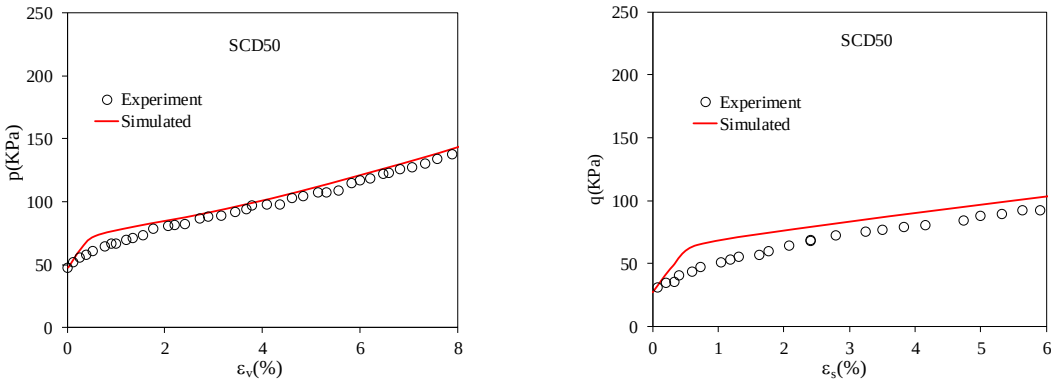

(a) p'-ε_v (b) q-ε_s

Fig. 6 Simulated and observed results of SCD50

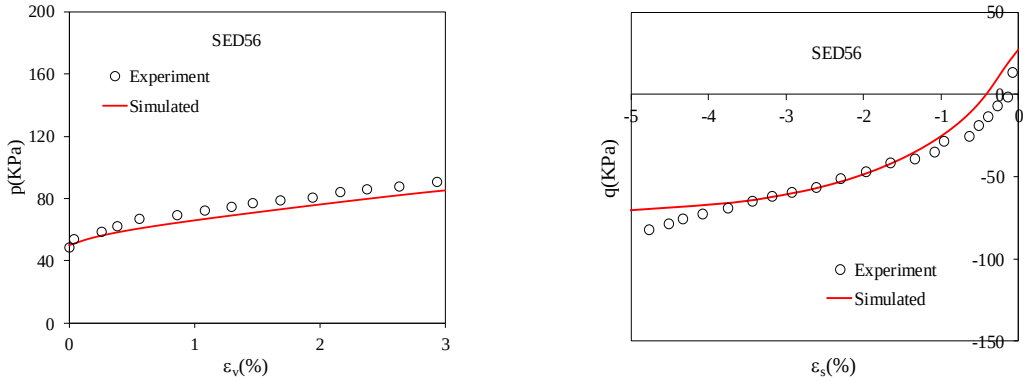

(a) p'-ε_v (b) q-ε_s

Fig. 7 Calculated and observed results of SED56

captures the stress-strain behavior very well. There exists a turning point, which is the characteristic for structured clay. Fig. 7 shows the simulated triaxial extension test results with the angle between stress path and p'-axis being 56 degree. The turning point of the simulated results under extension condition is not as obvious as the results under compression condition. This is due to the fact that structural of clay has less influence on the stress-strain behavior when loaded under extension condition compared to load under compression condition. In both compression and extension tests, the simulations capture the experimental behavior very well.

The triaxial undrained tests on Vallericca clay were carried out by Burland *et al*. (1996). In the tests, the clay sample was first anisotropically consolidated up to an effective stress of p'_{max} that is larger than p'_{yi}, and then the sample was swelled back to different OCRs. Results of the simulation using proposed model were shown in Fig. 8. It can be seen that although there are some discrepancies in the effective stress path results, in general, the simulated results agree with the experimental results very well. The dilatancy trend was well captured. Moreover, in the overconsolidation region, the peak strength line is exceeding the critical state line, which means that the overconsolidated clays are tougher than the reconstituted clays.

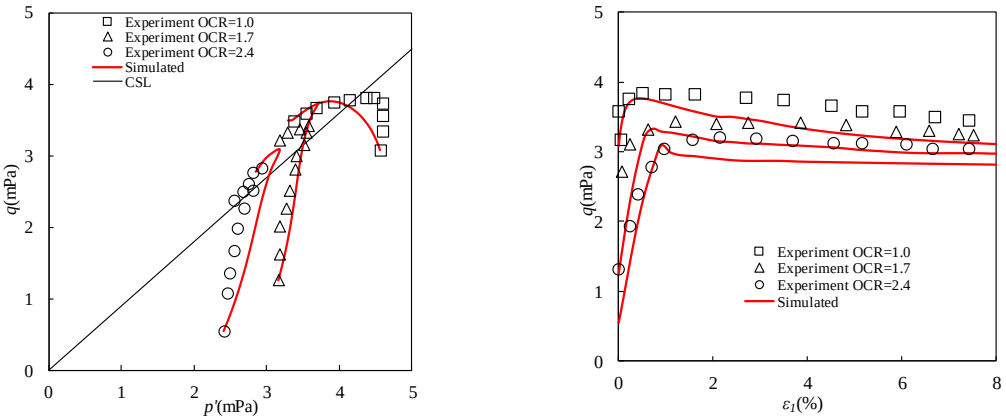

Fig. 8 Comparison between experimental and simulated results of Vallericca clay: (a) Effective stress paths; (b) Deviatoric stress versus axial strain

4. Numerical example – Murro test embankment

4.1 Murro test embankment

The proposed constitutive model is applied to simulate behavior of the Murro test embankment, which was constructed on a soft clay deposit in Finland in 1993 and has been analyzed in a number of previous studies (Karstunen and Yin 2010, Karstunen *et al*. 2005). The purpose of this numerical example is to demonstrate the applicability and capability of the proposed constitutive model, in particular, the effect of anisotropy and structural on the predicted embankment response. The embankment is 2 m high and 30 m long with a 1:2 slope. Dimension of the embankment is shown in Fig. 9(b). The embankment was constructed within 2 days. The instrumentation of Murro test embankment included 7 settlement plates (S1-S7), 2 inclinometers (I1-I2), 1 extensometer (E) and 8 pore pressure probes (U1-U8), the layout of which is shown in Fig. 9. More details on the embankment can be found in Karstunen and Yin (2010).

4.2 Model parameters for Murro clay

The embankment was constructed using crushed rock which was modeled using a linear elastic–perfectly-plastic Mohr Coulomb model. Model parameters have been calibrated as [21]: Young's modulus E = 40000 kN/m^2, Poisson ratio ν = 0.35, friction angle ϕ'_c = 40°, dilation angle ψ = 0° and unit weight γ = 19.6 kN/m^3, apparent cohesion c' = 2 kN/m^2.

The proposed constitutive model will be used to model the underlying soft clay. The values of clay parameters e_0, λ_i, λ_n, κ, k_h, k_v, p'_{yi}, α_0, Δe_i, M and ν were estimated from laboratory results on intact and reconstituted samples. These parameters have been determined by Karstunen and Yin (2010) from conventional triaxial and oedometer tests. Anisotropy parameter μ and β are obtained from Eqs. (5) and (4), structural parameters ξ and ξ_d are obtained from Eqs. (23) and (24) respectively. All the model parameters are summarized in Table 5.

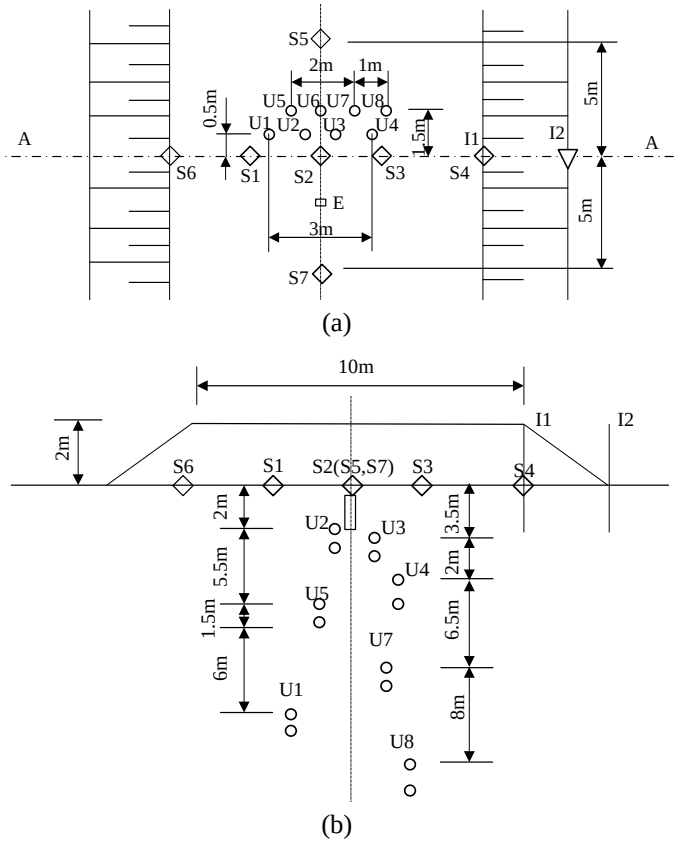

Fig. 9 Murro test embankment with details of instrumentation: (a) plan view; (b) profile view along A-A cross section

Table 5 Values of parameters for Murro clay

Depth (m)	γ (kN/m^3)	e_0	M	K_0	κ	λ_i	λ_n	ν	Δe_i
0.0-1.6	15.8	1.57	1.70	1.25	0.010	0.07	0.16	0.35	0.10
1.6-3.0	15.5	1.81	1.70	0.34	0.030	0.24	0.50	0.10	0.47
3.0-6.7	14.9	2.45	1.65	0.35	0.036	0.24	0.50	0.15	0.45
6.7-10.0	15.1	2.16	1.50	0.40	0.030	0.18	0.36	0.15	0.36
10.0-15.0	15.5	1.76	1.45	0.42	0.034	0.16	0.32	0.15	0.29
15.0-23.0	15.9	1.53	1.40	0.43	0.004	0.07	0.14	0.15	0.15

Depth (m)	ξ	ξ_d	μ	β	k_h (m/s)	k_v (m/s)
0.0-1.6	1.54	14.8	55	1.02	2.47E-09	1.90E-09
1.6-3.0	1.55	1.79	38	1.05	2.47E-0.9	1.90E-09
3.0-6.7	1.93	1.84	40	0.92	2.06E-09	1.55E-09
6.7-10.0	1.72	2.64	56	1.00	1.27E-09	1.05E-09
10.0-15.0	1.54	3.66	65	1.09	7.93E-10	6.34E-09
15.0-23.0	1.30	11.29	58	0.88	1.20E-09	9.51E-09

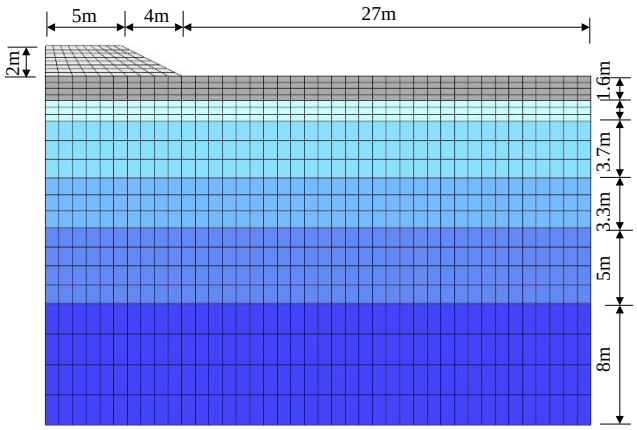

Fig. 10 Finite element mesh for Murro test embankment on soft clay

4.3 Finite element models

In the finite element method analysis, the plain strain condition was assumed and the finite element mesh is shown in Fig. 10. The groundwater table was located at a depth of 0.8 m. Vertical boundaries on both sides are restrained from moving horizontally, and the bottom boundary is restrained in both directions. Due to symmetry, only half of the embankment is represented in the finite element mesh. The finite element mesh is composed of 1256 elements with 2812 nodes, the element type above the ground table is CPE4, and CPE4P below the ground table.

Several locations for reporting settlement are monitored in the simulation, which correspond to S2, S4, S5, S6 and S7 in the field-monitoring plan. The location for reporting horizontal displacements is 5 m off the centerline which corresponds to inclinometer I1 in the field-monitoring plan.

The embankment loading was added within two days to mimic real construction. To illustrate the influence of different model features on the simulated embankment behavior, three scenarios are considered: (1) no anisotropy and structural features were turned on, which corresponds to ($\alpha_0 = \mu = \beta = 0$ and $\Delta e_i = \xi = \xi_d = 0$); (2) only anisotropy was included, which corresponds to ($\Delta e_i = \xi = \xi_d = 0$); and (3) both anisotropy and structural were activated, in which case the input parameters are the same as listed in Table 5.

4.4 Settlement and horizontal displacement

Fig. 11 shows the surface settlements under the centerline and 5 m off the centerline of the embankment by the proposed model with or without clay anisotropy and structural. It can be seen that the influence of anisotropy and structural is not very clear at the early stage. However, the difference among simulation results with or without clay anisotropy and structural become profound in the long-term. Clay anisotropy results in larger settlement than that in the isotropic case, then the destructuration further increases predicted the settlement. It shows the influence of anisotropy and structural influence on the settlement over the long term.

Fig. 12 shows the measured and simulated horizontal displacements immediately after construction and after 8 years, respectively. The influence of the two features on the horizontal displacement is similar to that on the settlement. Simulation without anisotropy and structural

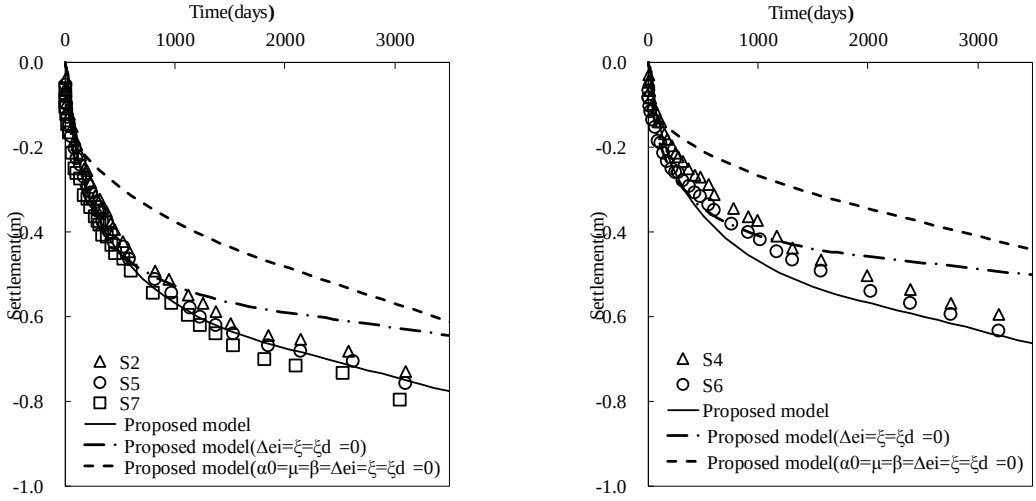

(a) Under the centerline (b) 5 m from centerline

Fig. 11 The settlement-time curves: (a) under the centerline; (b) 5 m from centerline

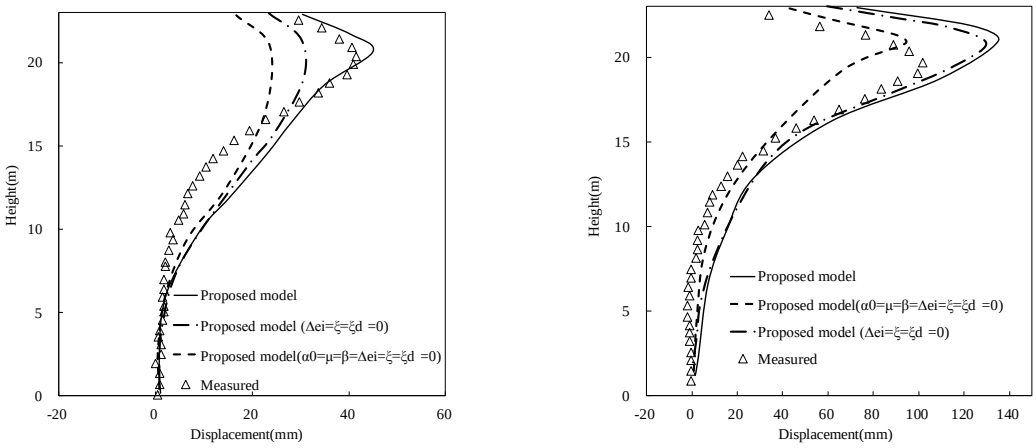

(a) Immediately after construction (b) After 8 years

Fig. 12 The measured and simulated horizontal displacements underneath crest of embankment slope

predicts the small horizontal displacements, then both anisotropy and structural increase the predicted horizontal displacement. The difference between the predicted results after 8 years is same as that at the end of construction, their differences is still obvious, but at the same time, the difference is decreasing with the increasing of the depth, at the depth of about 8 m after construction and 5 m after 8 years, the horizontal displacement is almost the same. The depth of the maximum horizontal displacement is well predicted in the three cases, it shows that anisotropy and structural have little influences on the depth of the maximum horizontal displacement.

Fig. 13 shows the evolution of the ratio of maximum horizontal displacement $U_{x\max}$ at I1 to the maximum settlement $U_{y\max}$ at centerline with time, comparing the model predictions with the field

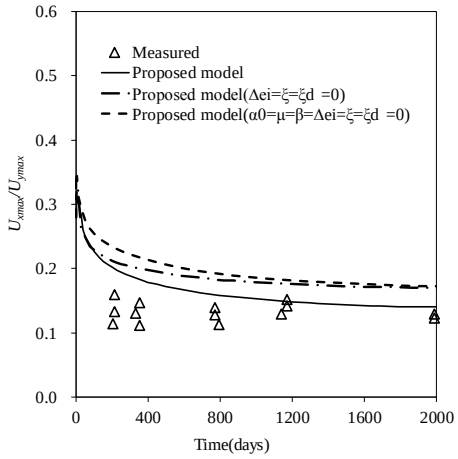

Fig. 13 The ratio of the maximum horizontal displacement and maximum settlement versus time

data, it can be seen there is a significant increase is noticed during the construction of embankment. When the construction is completed, the ratio between U_{xmax} and U_{ymax} decreases over time. Simulation without anisotropy and structural effects predicts the highest ratio, while simulations with anisotropy and structural predict the lowest ratio at the long term. The simulations both anisotropy and structural effects give the best matches to measurements in the three circumstance.

In order to establish the relationship between the maximum horizontal displacements and maximum settlement for convenient applications, filed data of maximum settlements and maximum horizontal displacement of 36 embankments (Saiichi and Takeshi 1996, Zhu and Yin 2000, Mestat 2001, Zdravkovic *et al*. 2002, Karstunen 2005, Karstunen *et al*. 2006, Abdulazim *et al*. 2008, Abdulazim 2009, Curtis *et al*. 2009, Karstunen and Yin 2010, Paulo *et al*. 2011, Karim *et al*. 2011) have been collected in this paper, the relationship between maximum settlements and maximum horizontal displacement is shown in Fig. 14.

The relation between the maximum horizontal displacements and the settlements at the end of construction can be expressed

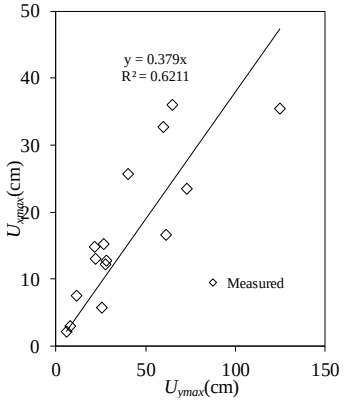

(a) At the end of construction

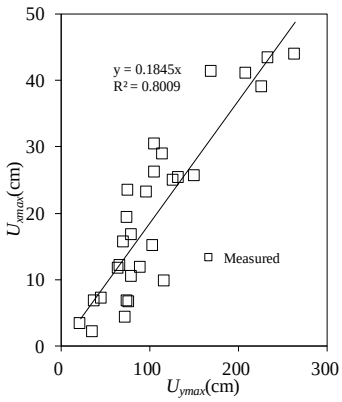

(b) Over the long term

Fig. 14 Relation between horizontal displacement and settlement

$$U_{x\max.} = 0.379U_{y\max} \tag{26}$$

Then when entering the consolidation stage, the maximum horizontal displacements and the settlements at the end of construction can be expressed:

$$U_{x\max.} = 0.184U_{y\max} \tag{27}$$

It can be seen that the simulated results have good agreement with Eqs. (26) and (27), it shows the prediction capability of this model.

5. Conclusions

In this paper, an elasto-plastic model able to capture the anisotropy and structural of natural soft clay is proposed. The yield surface of the proposed model is adapted from the anisotropic elasto-plastic S-CLAY1 model. The compression curve of reconstituted clays is taken as the reference to describe the structural of clay. There are 6 parameters which are similar to the S-CLAY1 model and 3 structural parameters. The model parameters all have clear physical meanings and can be determined in a relatively straightforward way. The model was then implemented into the finite element code for analyzing boundary value problem, including triaxial tests and an Murro embankment. The simulated results were compared with the measured data in terms of settlement and horizontal displacement. Comparisons showed the improvement of predicted performance by incorporating structural and anisotropy, demonstrating the importance of these two features on predicted clay behavior. The relation between the maximum horizontal displacements and the maximum settlements at the end of construction and over the long term has also been proposed and the influence of anisotropy and structural on this ratio has been found to be less significantly as compared to the settlement and horizontal displacements.

References

Abdulazim, Y., Minna, K. and Harald, K. (2008), "Effect of anisotropy and destructuration on behavior of Haarajoki test embankment", *Int. J. Geomech*., **9**(4), 153-168.

Abdulazim, Y. (2009), Numerical analyses of embankments on PVD improved soft clays. *Advances in Engineering Software*, **4**, 1047-1055.

Burland, J.B. (1990), "On the compressibility and shear strength of natural clays", *Geotechnique*, **40**(3), 329-378.

Burland, J.B., Rampello, S., Georgiannou, V.N. and Calabresi, G. (1996), "A laboratory study of the strength of four stiff clays", *Geotechnique*, **46**(3), 491-514.

Chai, J.C., Miura, N. and Zhu, H.H. (2004), "Compression and consolidation characteristics of structured natural clays", *Can. Geotech. J.*, **41**(6), 1250-1258.

Chen, B., Xu, Q. and Sun, D.A. (2014), "An elastoplastic model for structured clays", *Geomech. Eng., Int. J.*, **7**(2), 213-231.

Cheng, X.L. and Wang, J.H. (2016), "An elastoplastic bounding surface model for the cyclic undrained behaviour of saturated soft clays", *Geomech. Eng., Int. J.*, **11**(3), 325-343.

Cotecchia, F. and Chandler, R.J. (2000), "A general framework for the mechanical behavior of clays", *Geotechnique*, **50**(4), 431-447.

Curtis, K., Jitendra, S., David, H. and James, G. (2009), "Finite element analysis of an embankment on a soft estuarine deposit using elastic-viscoplastic soil model", *Can. Geotech. J.*, **46**(3), 357-368.

Dafalias, Y.F. (1986), "Bounding surface plasticity: Mathematical foundation and hypoplasticity", *J. Eng. Mech.*, **112**(9), 966-987.
Dafalias, Y.F. (1987), "Anisotropic critical state clay plasticity model", *Proceedings of the 2nd International Conference on Constitutive Laws for Engineering Materials*, Volume 1, Tucson, AZ, USA, pp. 513-521.
Gajo, A. and Wood, D.M. (2001), "A new approach to anisotropic, bounding surface plasticity: general formulation and simulations of natural and reconstituted clay behaviour", *Int. J. Numer. Anal. Method. Geomech.*, **25**(3), 207-241.
Gens, A. and Nova, R. (1993), "Conceptual bases for a constitutive model for bonded soils and weak rocks", *Proceedings of International Symposium on Hard Soils - Soft Rocks*, Athens, Greece, September, pp. 485-494.
Huang, M.S., Liu, Y.H. and Sheng, D.C. (2011), "Simulation of yielding and stress-strain behavior of Shanghai soft clay", *Comput. Geotech.*, **38**(3), 341-353.
Jirayut, S., Suksun, H. and Martin, D.L. (2010), "Modified structured cam clay: A generalised critical state model for destructured, naturally structured and artificially structured clays", *Comput. Geotech.*, **37**(7), 956-968.
John, P., Carter, J.P. and Martin, D. (2005), "Review of the structured cam clay model", In: *Soil Constitutive Models*: *Evaluation, Selection, and Calibration*, **128**, 99-132.
Karim, M.R., Manivannan, G., Gnanendran, C.T. and Lo, S.C.R. (2011), "Predicting the long-term performance of a geogrid-reinforced embankment on soft soil using two-dimensional finite element analysis", *Can. Geotech. J.*, **48**(5), 741-753.
Karstunen, M. and Yin, Z.Y. (2010), "Modelling time-dependent behavior of Murro test embankment", *Geotechnique*, **60**(10), 735-749.
Karstunen, M., Krenn, H., Wheeler, S.J., Koskinen, M. and Zentar, R. (2005), "Effect of anisotropy and destructuration on the behavior of Murro test embankment", *Int. J. Geomech.*, **5**(2), 87-97.
Karstunen, M., Wiltafsky, C., Krenn, H., Scharinger, F. and Schweiger, H.F. (2006), "Modelling the behaviour of an embankment on soft clay with different constitutive models", *Int. J. Numer. Anal. Method. Geomech.*, **30**(10), 953-982.
Kavvadas, M. and Amorosi, A. (2000), "A constitutive model for structured soils", *Geotechnique*, **50**(3), 263-273.
Kimoto, S. and Oka, F. (2005), "An elasto-viscoplastic model for clay considering destructuralization and consolidation analysis of unstable behavior", *Soils Found.*, **45**(2), 29-42.
Koskinen, M., Karstunen, M. and Wheeler, S.J. (2002), "Modelling destructuration and anisotropy of a natural soft clay", *Proceeding of the 5th European Conference on Numerical Methods in Geotechnical Engineering*, Paris, France, September, pp. 11-20.
Leroueil, S. and Vaughan, P.R. (1990), "The general and congruent effects of structure in natural soils and week rock", *Geotechnique*, **40**(3), 467-488.
Leroueil, S., Tavenas, F. and Brucy, F. (1979), "Behavior of destructured natural clays", *J. Geotech. Eng. Div.*, **105**(6), 759-778.
Liu, M.D. and Carter, J.P. (2000), "Modeling the destructuring of soils during virgin compression", *Geotechnique*, **50**(4), 479-483.
Liu, M.D. and Carter, J.P. (2002), "A structured cam clay model", *Can. Geotech. J.*, **39**(6), 1313-1332.
Locat, J. and Lefebvre, G. (1985), "The compressibility and sensitivity of an artificially sedimented clay soil: the Grande-Baleine marine clay", *Marine Georesour. Geotech.*, **6**(1), 1-27.
Marcin, C. and Pieter, A.V. (2004), "On the modelling of anisotropy and destructuration of soft clays within the multi-laminate framework", *Comput. Geotech.*, **31**(1), 1-22.
Mestat, P.H. (2001), "MOMIS: une base de donnees sur la modelisation numerique des remblais sur sols compressibles et sur la confrontation calculs–mesures in situ", *Bulletin des Laboratories des Ponts et Chaussees*, **232**, 43-58.
Nakano, M., Nakai, K., Noda, T. and Asaoka, A. (2005), "Simulation of shear and one-dimensional compression behavior of naturally deposited clays by super/subloading yield surface Cam-clay model", *Soils Found.*, **45**(1), 141-151.

Ng, C.W.W., Li, Q. and Liu, G.B. (2011), "Characteristics of one-dimensional compressibility of Shanghai clay", *Chinese J. Geotech. Eng.*, **33**(4), 630-636. [In Chinese]
Paulo, J., Venda, O. and Luis, J.L. (2011), "Numerical predictions of the behaviour of soft clay with two anisotropic elastoplastic models", *Comput. Geotech.*, **38**(5), 598-611.
Pietruszczak, S. and Pande, G.N. (2001), "Description of soil anisotropy based on multi-laminate framework", *Int. J. Numer. Anal. Methods Geomech.*, **25**(2), 197-206.
Saiichi, S. and Takeshi, K. (1996), "Simplified deformation analysis for embankment foundation using elasto-plastic model", *Soils Found.*, **36**(2), 1-11.
Sheng, D., Sloan, S.W. and Yu, H.S. (2000), "Aspects of finite element implementation of critical state models", *Computat. Mech.*, **26**(2), 185-196.
Vincenzo, S. and Ghassan, A.S. (2009), "Analytical solution of stress-strain relationship of modified Cam clay in undrained shear", *Geomech. Eng., Int. J.*, **1**(4), 263-274.
Wheeler, S.J., Naatanen, A., Karstunen, M. and Lojander, M. (2003), "An anisotropic elastoplastic model for soft clay", *Can. Geotech. J.*, **40**(2), 403-418.
Whittle, A.J. and Kavvadas, M.J. (1994), "Formulation of MIT-E3 constitutive model for overconsolidated clays", *J. Geotech. Eng.*, **120**(1), 173-198
Yin, J. (2012), "Effect of soil structure on compression behavior of natural soft clays", *Chinese J. Rock Soil Mech.*, **33**(1), 48-52. [In Chinese]
Yin, Z.Y., Chang, C.S., Karstunen, M.H. and Hicher, P.V. (2010), "An anisotropic elastic–viscoplastic model for soft clays", *Int. J. Solids Struct.*, **47**(5), 665-677.
Zdravkovic, L., Potts, D.M. and Hight, D.W. (2002), "The effect of strength anisotropy on the behavior of embankments on soft clay", *Geotechnique*, **52**(6), 447-457.
Zhu, G.F. and Yin, J.H. (2000), "Elastic visco-plastic consolidation modelling of clay foundation at Berthierville test embankment", *Int. J. Numer. Anal. Method. Geomech.*, **24**(5), 491-508.

CC